Supplementary information for

CARIMED (CARbon, tracers, and ancillary data In the MEDiterranean Sea): A ship-based data synthesis product – overview and quality control procedures

Marta Álvarez[1], Maribel I. García-Ibáñez[2,3], Nico Lange[4,5], Alex Kozyr[6], Antón Velo[7], Toste Tanhua[4], Giuseppe Civitarese[8], Carolina Cantoni[9], Malek Belgacem[9], Katrin Schroeder[9], Rubén Acerbi[1], Laurent Coppola[10], Thibaut Wagener[11], Noelia M. Fajar[12], Susana Flecha[13], Michele Giani[8], Louisa Giannoudi[14], Elisa F. Guallart[3], Abed El Rahman Hassoun[3,15], Emma I. Huertas[13], Valeria Ibello[9,16], Mehdia A. Keraghel[17], Férial Louanchi[17], Anna Luchetta[9], Fiz F. Pérez[7], Carsten Schirnick[4], Ekaterini Souvermezoglou[14], Lidia Urbini[8], Monserrat Vidal[18], Patrizia Ziveri[19,20,21]

[1]Centro Oceanográfico de A Coruña (COAC-IEO), CSIC, A Coruña, 15001, Spain
[2]Centro Oceanográfico de Baleares (COB-IEO), CSIC, Palma de Mallorca, 07015, Spain
[3]Institut de Ciències del Mar (ICM), CSIC, Barcelona, Spain
[4]GEOMAR Helmholtz Centre for Ocean Research Kiel, Kiel, Germany
[5]NORCE Norwegian Research Centre, Bjerknes Centre for Climate Research, Bergen, Norway
[6]OCADS, National Centers for Environmental Information, National Oceanic and Atmospheric Administration, U.S.A.
[7]Instituto de Investigaciones Marinas (IIM), CSIC, Vigo, 36208, Spain
[8]OGS-National Institut of Oceanography and Applied Geophysics, Trieste, Italy
[9]Consiglio Nazionale delle Ricerche-Istituto di Scienze Marine (CNR-ISMAR), Trieste/Venezia, Italy
[10]Sorbonne Université, CNRS, UMR 7093, Laboratoire d'Océanographie de Villefranche-sur-Mer (LOV), Villefranche-sur-Mer, France
[11]Aix Marseille Université, CNRS, IRD, MIO, Marseille, France
[12]Centro Oceanográfico de Vigo (COV-IEO), CSIC, Vigo, Spain
[13]Instituto de Ciencias Marinas de Andalucía (ICMAN), CSIC, Puerto Real, Cádiz, Spain
[14]Hellenic Centre for Marine Research, HCMR, Anavissos, Greece
[15]National Council for Scientific Research, National Center for Marine Sciences, Beirut, Lebanon
[16]Middle East Technical University, Institute of Marine Sciences, Mersin, Turkey
[17]Ecole Nationale Supérieure des Sciences de la Mer et de l'Aménagement du Littoral, ENSSMAL, Algiers, Algeria
[18]Universitat de Barcelona (UB), Barcelona, Spain
[19]Institute of Environmental Science and Technology (ICTA-UAB), Universitat Autònoma de Barcelona, Bellaterra, Spain
[20]Catalan Institution for Research and Advanced Studies (ICREA), Barcelona, Spain
[21]Department of Animal Biology, Plant Biology and Ecology (BABVE), Universitat Autònoma de Barcelona, Bellaterra, Spain

Correspondence to: Marta Álvarez (marta.alvarez@ieo.csic.es)

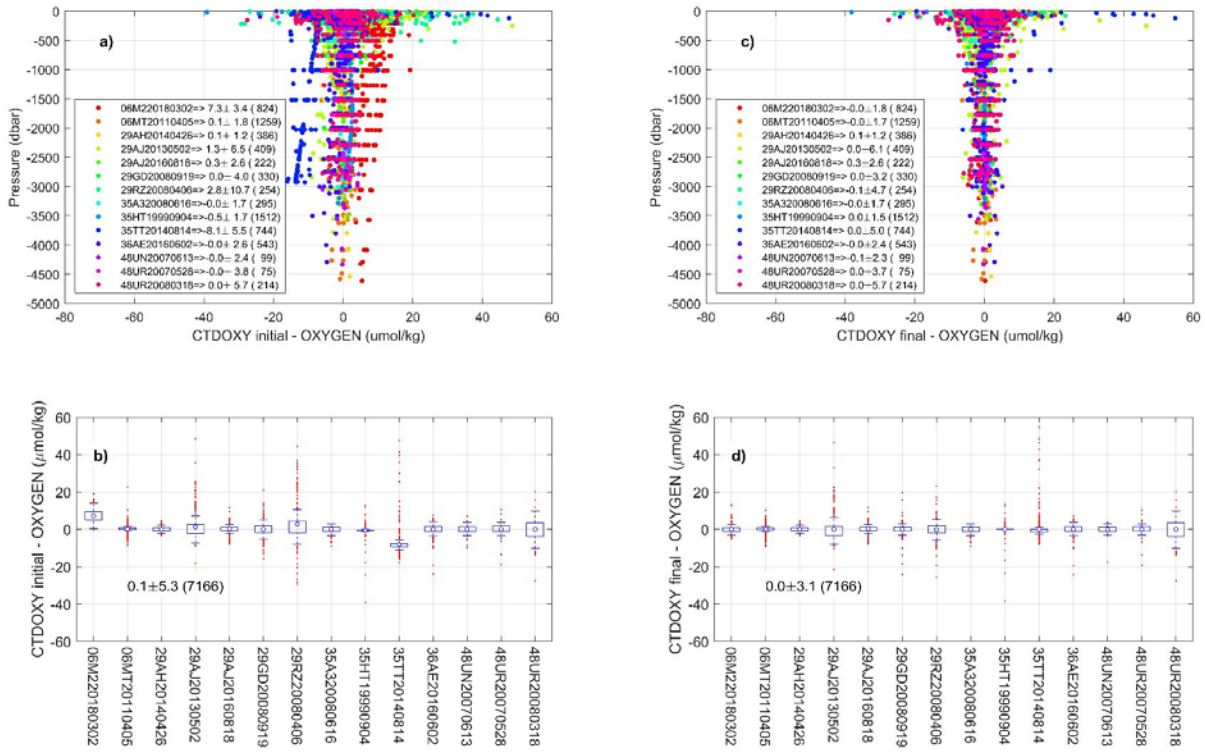

Figure S1. Primary quality control of sensor-based dissolved oxygen (CTDOXY) against discrete Winkler oxygen (OXYGEN). The figure illustrates the difference (CTDOXY-OXYGEN) before and after recalibration: (a) and (c) are scatter plots of the difference versus pressure, coloured by cruise. Cruise legends indicate the mean, standard deviation, and number of samples for the difference for each cruise (identified by its EXPOCODE). (b) and (d) are box-and-whisker plots showing the CTDOXY-OXYGEN differences grouped by cruise, before (b) and after (d) recalibration. In these plots, large red dots represent the cruise mean, small red dots denote outliers, and the overall mean and standard deviation are numerically indicated.

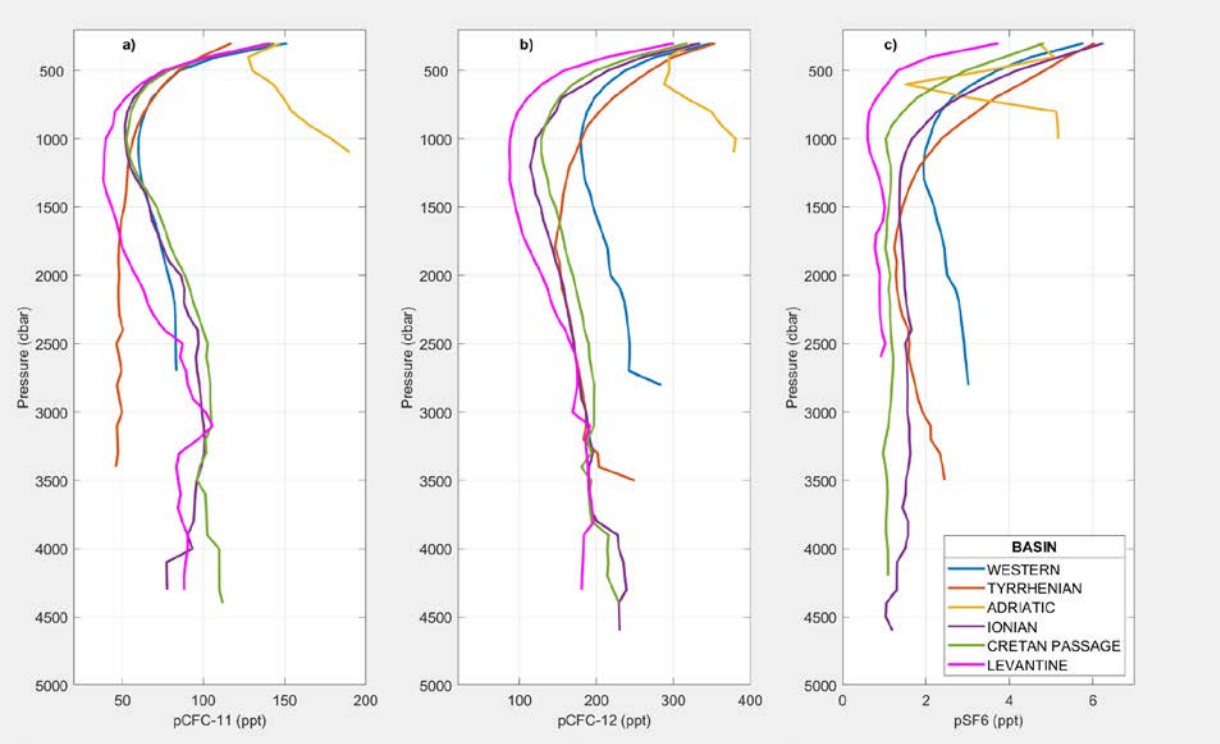

Figure S2. Mean vertical profiles for the partial pressure of a) CFC-11, b) CFC-12, and c) SF_6 (all in parts per trillion, ppt) in the different Mediterranean Sea sub-basins using the CARIMED transient tracer dataset. The profiles are segregated by sub-basin region (Fig. S3): Western Mediterranean Basin comprises regions DF1 (Algero-Provençal) and DS1 (Alboran Sea), Tyrrhenian Basin comprises regions DT1 (Tyrrhenian North) and DT3 (Tyrrhenian South), Ionian Basin comprises regions DJ5, DJ7, and DJ8 (Ionian South, Ionian Middle West, and Ionian Middle East, respectively), Cretan Passage comprises region DH3 (Cretan Passage), and Levantine Basin comprises regions DL1, DL2, DL3, and DL4 (Levantine North, Levantine North-East, Levantine South, and Levantine South-East, respectively).

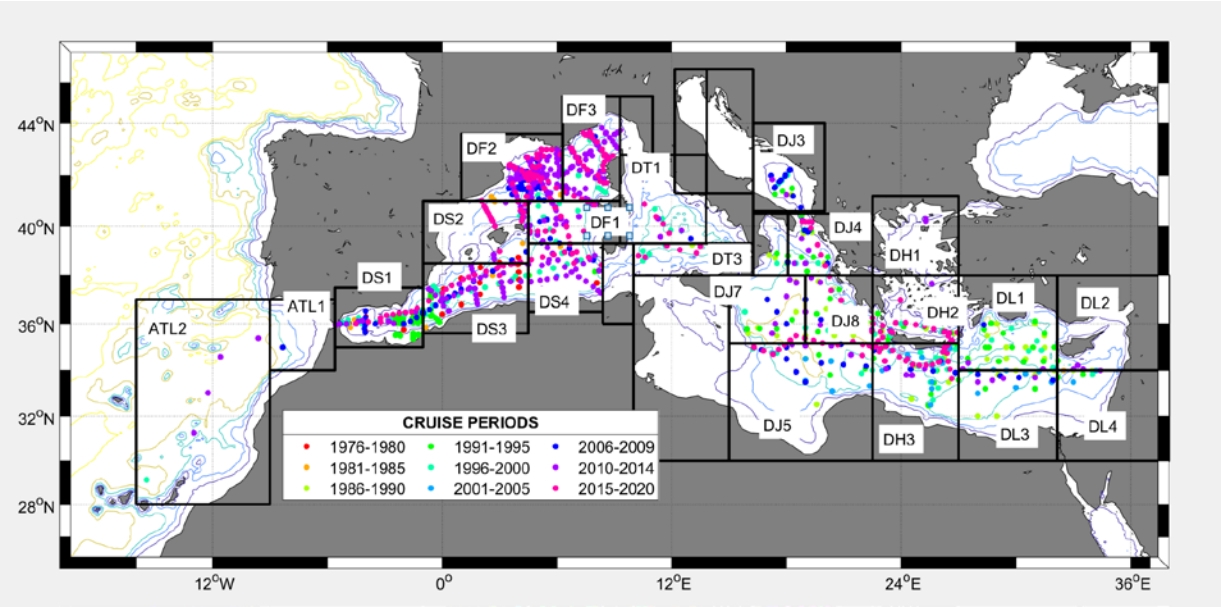

Figure S3. Map of the Mediterranean Sea showing the locations of the stations compiled in CARIMED that complied with the vertical pressure criteria used within the CARIMED 2QC framework, correspondingly divided into regional areas according to Manca et al. (2004). See Table S3 for more information.

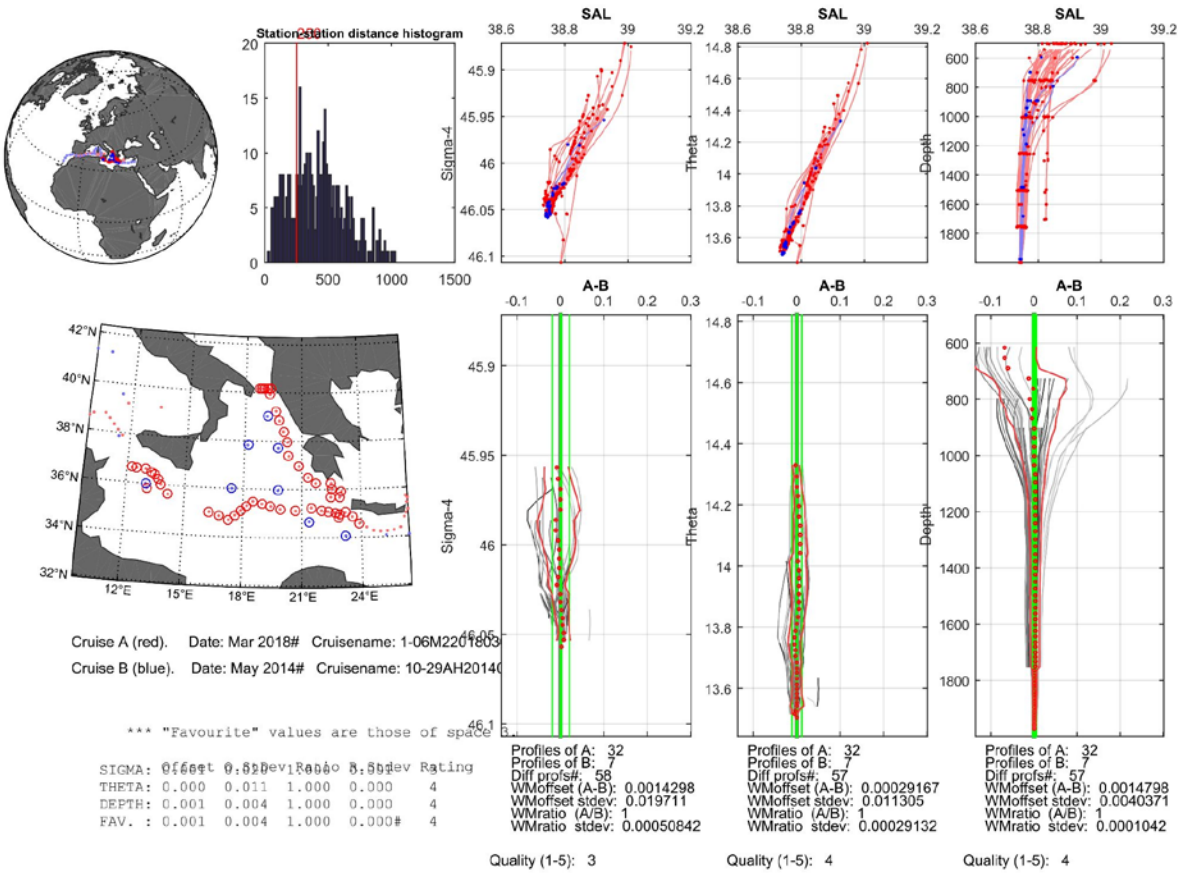

Figure S4. Additive salinity offset detected between the target cruise 06M220180302 (red) and the reference cruise 29AH20140426 (blue) in the Ionian Basin, illustrating a strong agreement between the two cruises, i.e., no adjustment required. The figure panels provide a complete overview of the crossover procedure: the top left panel shows the map of the full cruise transects, indicating spatial context, along with a histogram of the station-to-station distances (where the average distance is marked by a vertical red line); the bottom left panel displays the specific stations utilised for the crossover analysis; the top right panels present the measured vertical profiles of salinity for both cruises; and the bottom right panels display the differences between the two profiles (dotted red line) and the weighted average of these differences (solid green line), which represents the calculated offset. Statistical summaries and details of the analysis are provided in the bottom left corner and immediately beneath the profile difference panels.

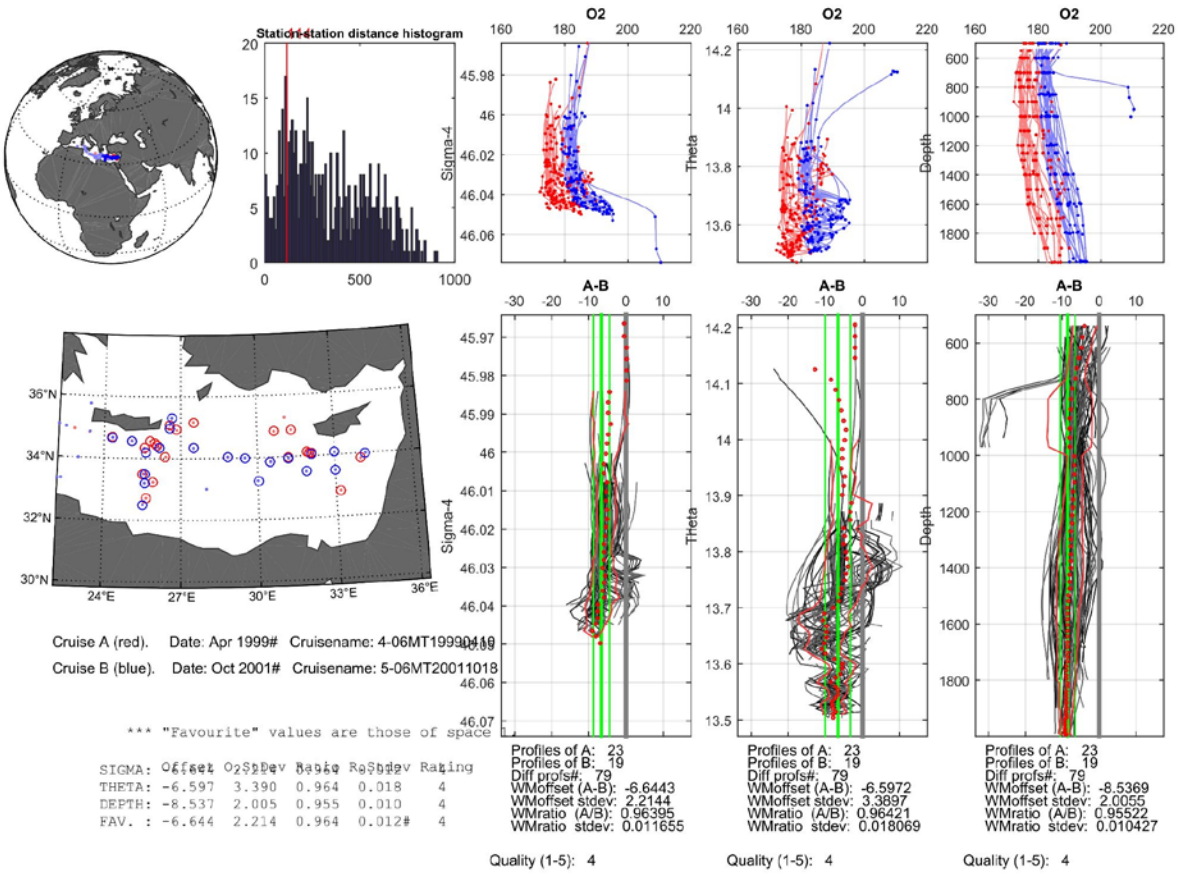

Figure S5. Multiplicative oxygen offset detected between the target cruise 06MT19990410 (red) and the reference cruise 06MT20011018 (blue) in the Levantine Basin. The crossover analysis indicates that the oxygen values for cruise 06MT19990410 need to be increased by approximately 3% compared to 06MT20011018, requiring a multiplicative adjustment of about 1/0.97=1.03. The figure panels provide a complete overview of the crossover procedure: the top left panel shows the map of the full cruise transects, indicating spatial context, along with a histogram of the station-to-station distances (where the average distance is marked by a vertical red line); the bottom left panel displays the specific stations utilised for the crossover analysis; the top right panels present the measured vertical profiles of salinity for both cruises; and the bottom right panels display the differences between the two profiles (dotted red line) and the weighted average of these differences (solid green line), which represents the calculated offset. Statistical summaries and details of the analysis are provided in the bottom left corner and immediately beneath the profile difference panels.

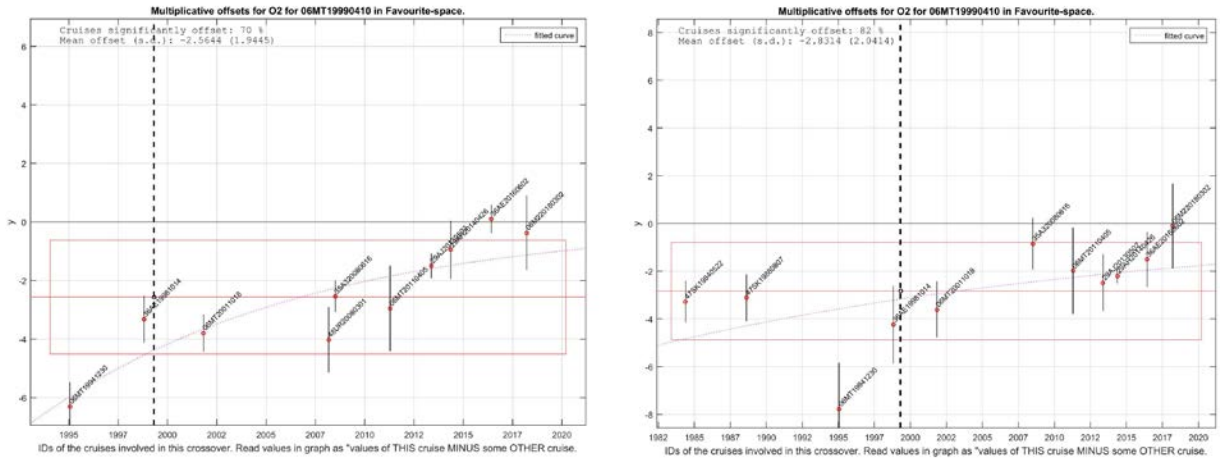

Figure S6. Weighted mean and standard deviation of the oxygen multiplicative offsets for the target cruise 06MT19990410 relative to its crossover cruises in the Ionian (left panel) and Levantine (right panel) Basins. The analysis, illustrating the average deviation in the favourite crossover space, highlights a potential adjustment of -3% when compared with cruises sampled close in time. Notably, the figure demonstrates a temporal trend in the Ionian Basin and a distinct regime shift evident in the Levantine Basin.

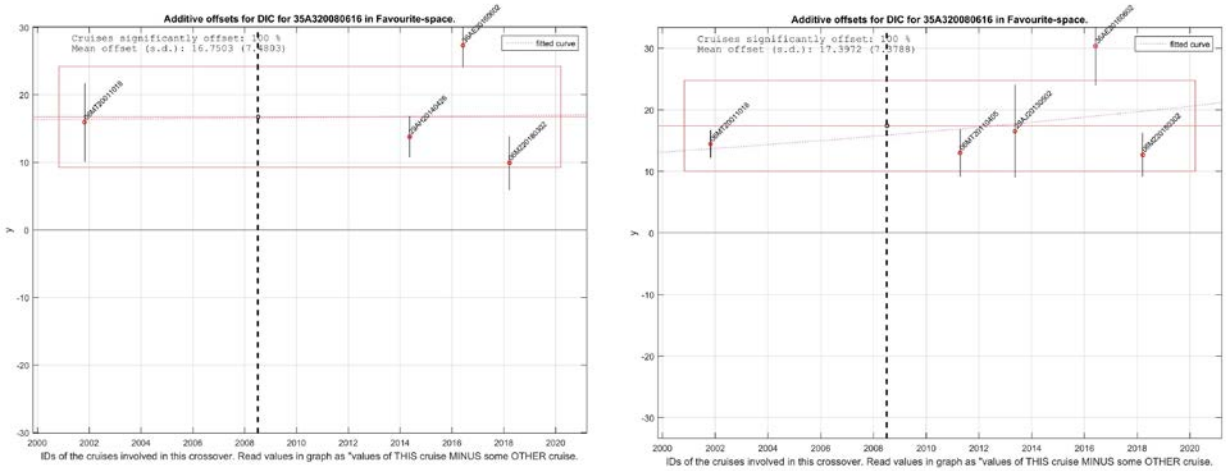

Figure S7. Weighted mean and standard deviation of the DIC additive offsets for the target cruise 35A320080616 relative to its crossover cruises in the Ionian (left panel) and Levantine (right panel) Basins. The analysis, illustrating the average deviation in the favourite crossover space, highlights a potential adjustment of about -10 µmol kg^{-1} in both basins.

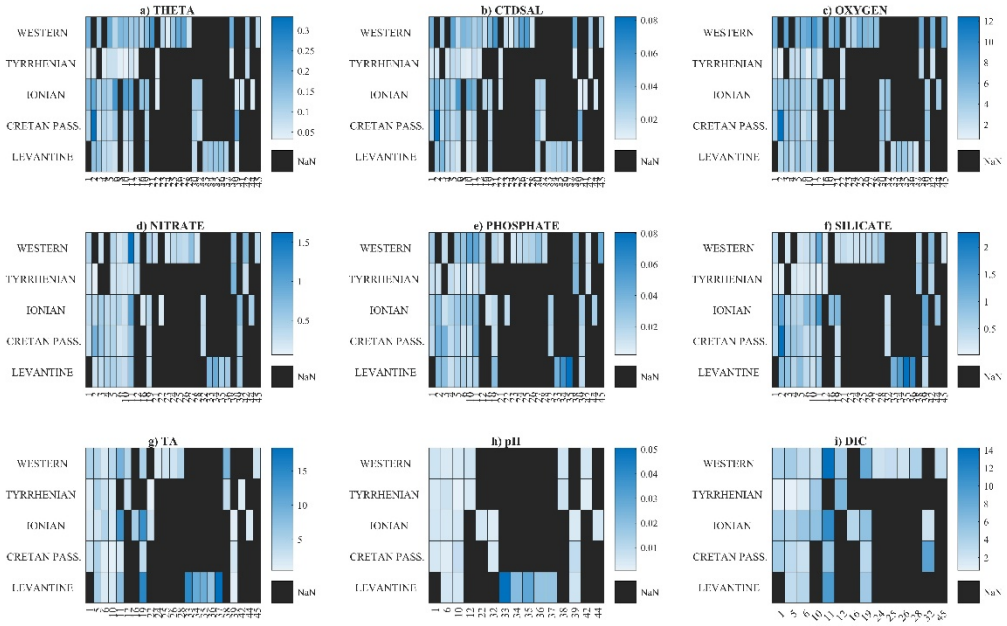

Figure S8. Heatmap illustrating the standard deviation of physical and biogeochemical variables, calculated for the depth layer with minimum temporal variability (Section 5.1), across each cruise included in CARIMED and grouped by sub-basin regions. This figure provides a preliminary inspection of the intra-cruise homogeneity (precision). The Mediterranean regions are grouped as follows: the Western Basin comprises regions DF1 (Algero-Provençal) and DS1 (Alboran Sea), the Tyrrhenian Basin comprises regions DT1 (Tyrrhenian Sea North) and DT3 (Tyrrhenian Sea South), the Ionian Basin comprises regions DJ5, DJ7, and DJ8 (Ionian South, Middle East, and West, respectively), the Cretan Passage comprises region DH3 (Cretan Passage), and the Levantine Basin comprises regions DL1, DL2, DL3, and DL4 (Levantine North, North East, South, and South East, respectively). Cruises can be identified by their cruise number using Tables 1 and S2. The variables depicted are: a) potential temperature (THETA in ºC), b) salinity (CTDSAL), c) dissolved oxygen (OXYGEN in µmol kg^{-1}), d to f) dissolved inorganic nutrients (all in µmol kg^{-1}), g) total alkalinity (TA in µmol kg^{-1}), h) pH on the total hydrogen ion scale at 25ºC (pH), and i) total dissolved inorganic carbon (DIC in µmol kg^{-1}).

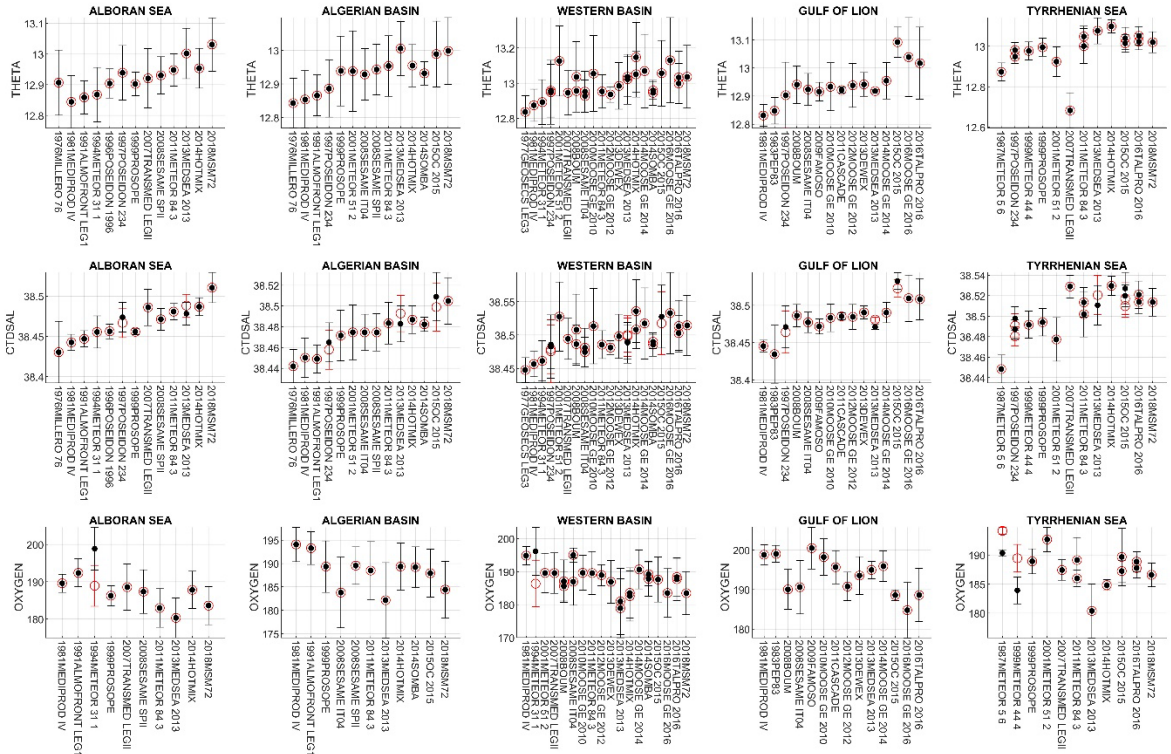

Figure S9. Mean and standard deviation values for physical and biogeochemical variables, calculated for the depth layers with minimum temporal variability (Section 5.1), CARIMED cruise and Mediterranean Sea grouped sub-basin regions according to Manca et al. (2004) classification (Fig. S3 and Table S3). The Alboran Sea comprises region DS1; the Algerian Basin comprises region DS3 (Algerian West); the Western Basin comprises regions DF1 (Algero-Provençal) and DS1 (Alboran Sea); the Gulf of Lion comprises region DF2; the Tyrrhenian Basin comprises regions DT1 (Tyrrhenian North) and DT3 (Tyrrhenian South). Cruises can be identified with the cruise number in Table 1 and S2. Variables are potential temperature (THETA in ºC), salinity, and dissolved oxygen (in µmol kg^{-1}). Black dots correspond to the original data, red circles are bias-corrected data.

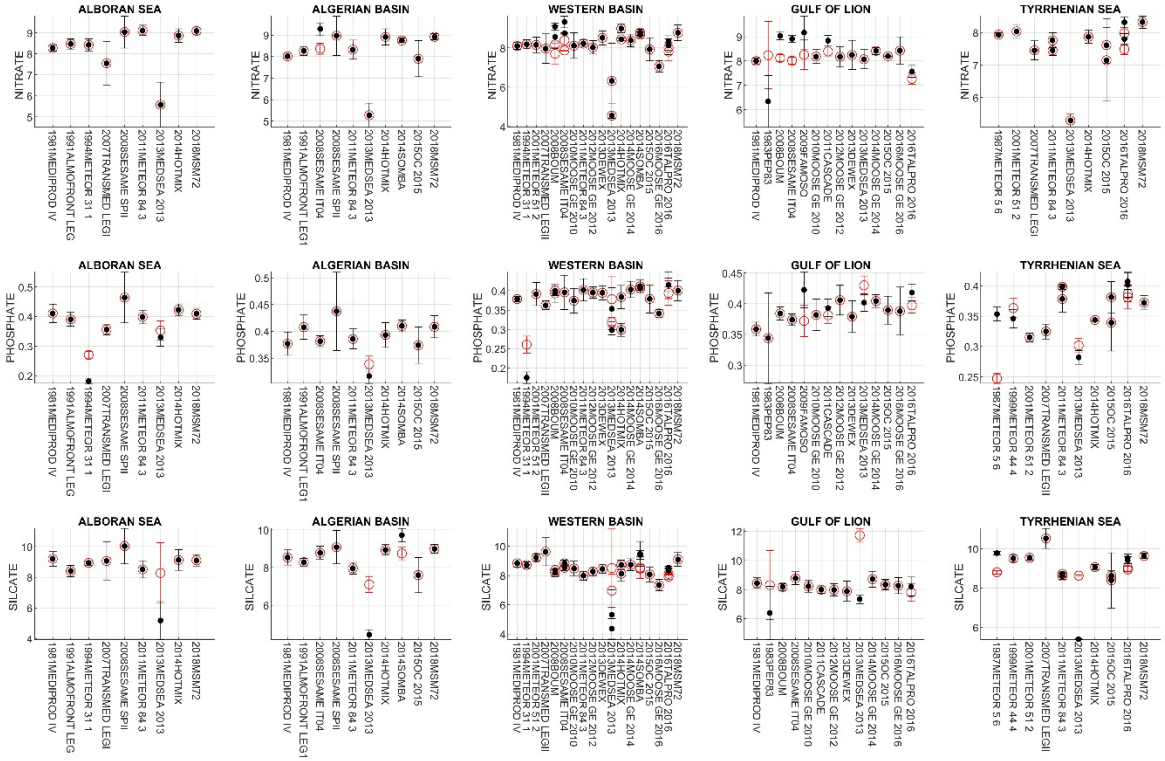

Figure S10. Mean and standard deviation values for physical and biogeochemical variables, calculated for the depth layers with minimum temporal variability (Section 5.1), CARIMED cruise and Mediterranean Sea grouped sub-basin regions according to Manca et al. (2004) classification (Fig. S3 and Table S3). The Alboran Sea comprises region DS1; the Algerian Basin comprises region DS3 (Algerian West); the Western Basin comprises regions DF1 (Algero-Provençal) and DS1 (Alboran Sea); the Gulf of Lion comprises region DF2; the Tyrrhenian Basin comprises regions DT1 (Tyrrhenian North) and DT3 (Tyrrhenian South). Cruises can be identified with the cruise number in Table 1 and S2. Variables are dissolved inorganic nutrients: nitrate, phosphate, and silicate (all in µmol kg^{-1}). Black dots correspond to the original data, red circles are bias-corrected data.

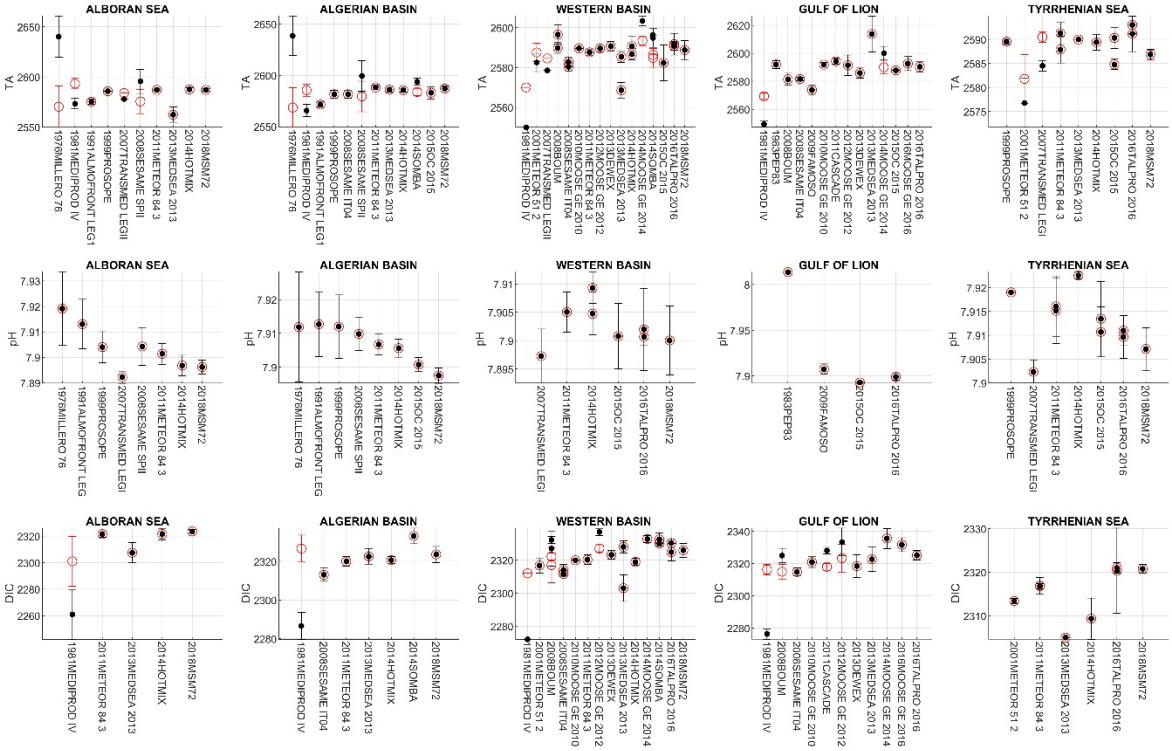

Figure S11. Mean and standard deviation values for physical and biogeochemical variables, calculated for the depth layers with minimum temporal variability (Section 5.1), CARIMED cruise and Mediterranean Sea grouped sub-basin regions according to Manca et al. (2004) classification (Fig. S3 and Table S3). The Alboran Sea comprises region DS1; the Algerian Basin comprises region DS3 (Algerian West); the Western Basin comprises regions DF1 (Algero-Provençal) and DS1 (Alboran Sea); the Gulf of Lion comprises region DF2; the Tyrrhenian Basin comprises regions DT1 (Tyrrhenian North) and DT3 (Tyrrhenian South). Cruises can be identified with the cruise number in Table 1 and S2. Variables are total alkalinity (TA in µmol kg^{-1}), pH on the total hydrogen ion scale at 25°C (pH), and total dissolved inorganic carbon (DIC in µmol kg^{-1}). Black dots correspond to the original data, red circles are bias-corrected data.

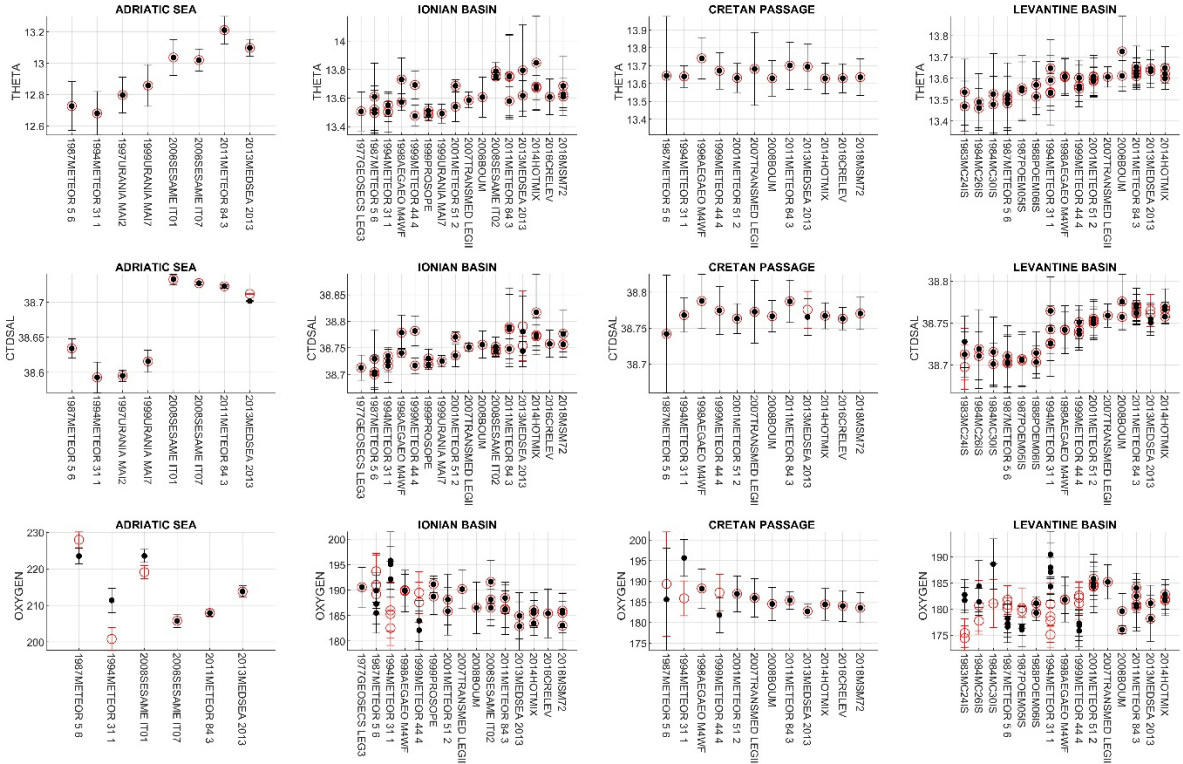

Figure S12. Mean and standard deviation values for physical and biogeochemical variables, calculated for the depth layers with minimum temporal variability (Section 5.1), CARIMED cruise and Mediterranean Sea grouped sub-basin regions according to Manca et al. (2004) classification (Fig. S3 and Table S3). The Adriatic Basin comprises region DJ3 (Adriatic South); the Ionian Basin comprises regions DJ5, DJ7, and DJ8 (Ionian South, Ionian Middle West, and Ionian Middle East, respectively); the Cretan Passage region comprises region DH3 (Cretan Passage), and the Levantine Basin comprises regions DL1, DL2, DL3, and DL4 (Levantine North, Levantine North-East, Levantine South, and Levantine South-East, respectively). Cruises can be identified with the cruise number in Table 1 and S2. Variables are potential temperature (THETA in ºC), salinity, and dissolved oxygen (in µmol kg^{-1}). Black dots correspond to the original data, red circles are bias-corrected data.

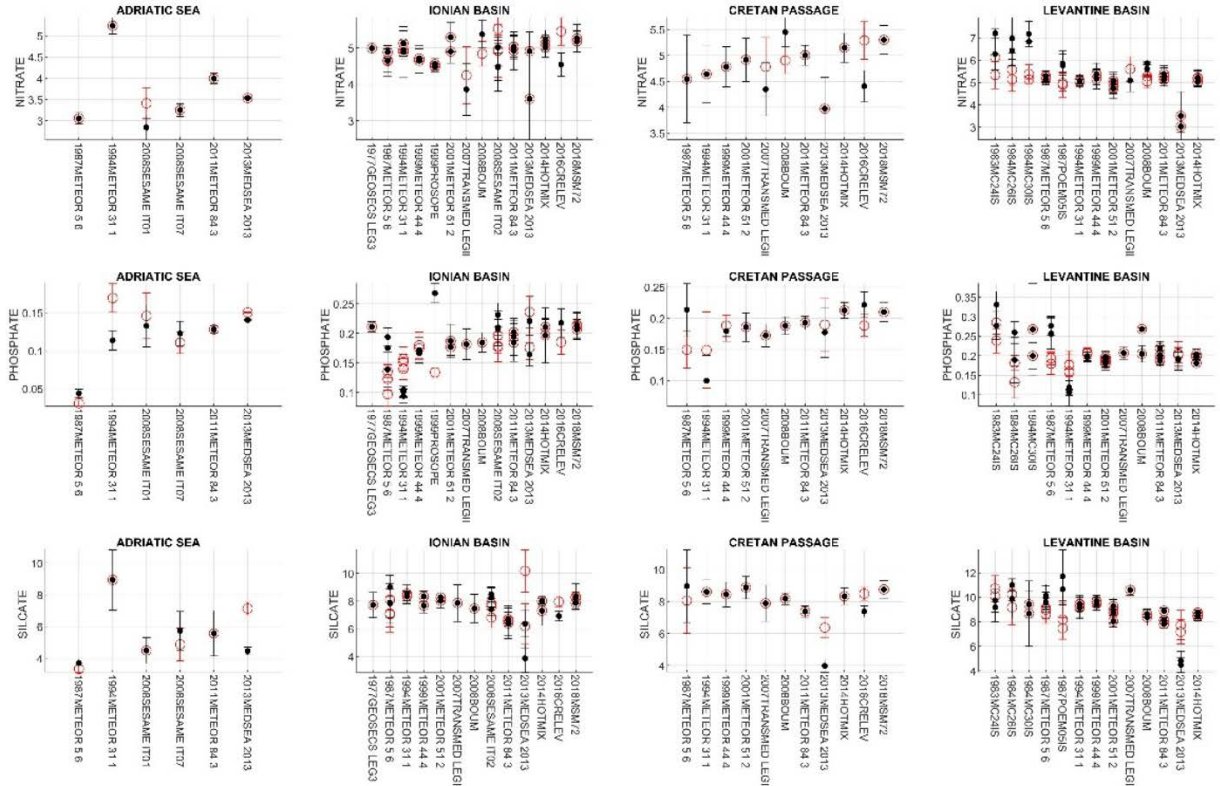

Figure S13. Mean and standard deviation values for biogeochemical variables, calculated for the depth layers with minimum temporal variability (Section 5.1), CARIMED cruise and Mediterranean Sea grouped sub-basin regions according to Manca et al. (2004) classification (Fig. S3 and Table S3). The Adriatic Basin comprises region DJ3 (Adriatic South); the Ionian Basin comprises regions DJ5, DJ7, and DJ8 (Ionian South, Ionian Middle West, and Ionian Middle East, respectively); the Cretan Passage region comprises region DH3 (Cretan Passage), and the Levantine Basin comprises regions DL1, DL2, DL3, and DL4 (Levantine North, Levantine North-East, Levantine South, and Levantine South-East, respectively). Cruises can be identified with the cruise number in Table 1 and S2. Variables are dissolved inorganic nutrients: nitrate, phosphate, and silicate (all in µmol kg^{-1}). Black dots correspond to the original data, red circles are bias-corrected data

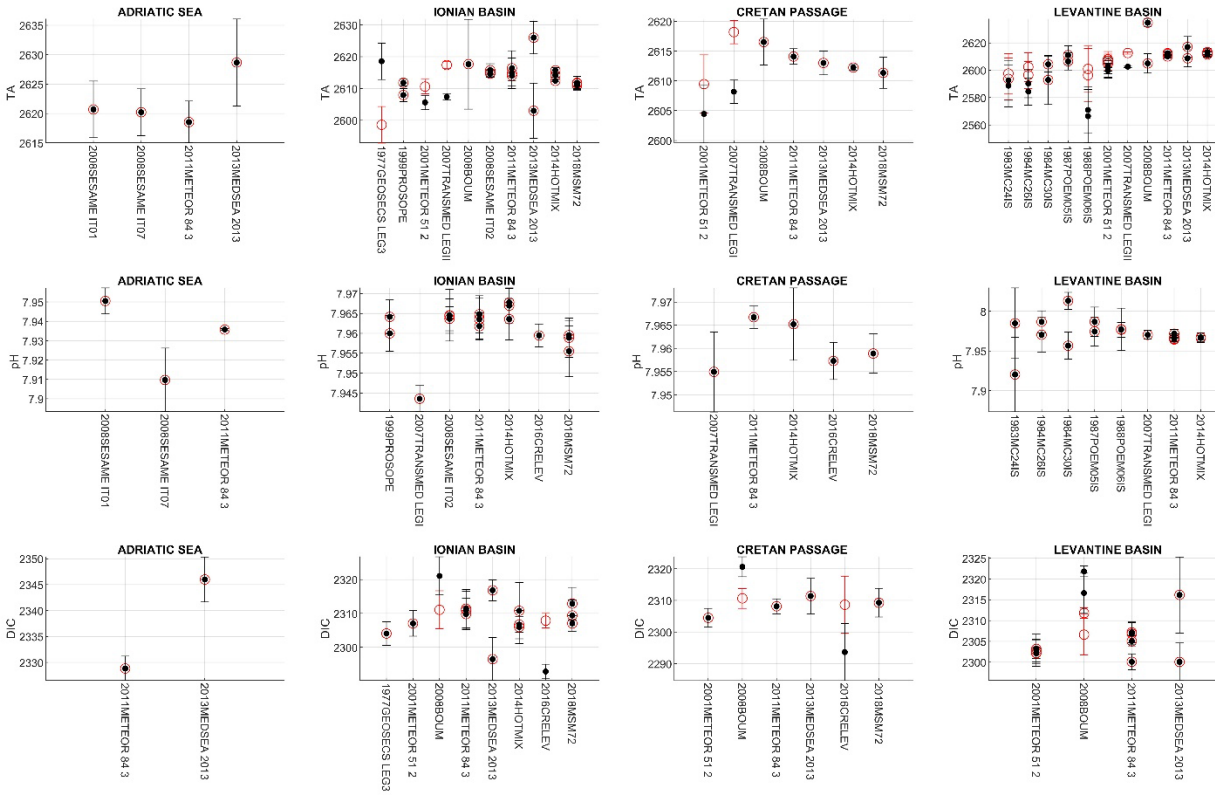

Figure S14. Mean and standard deviation values for biogeochemical variables, calculated for the depth layers with minimum temporal variability (Section 5.1), CARIMED cruise and Mediterranean Sea grouped sub-basin regions according to Manca et al. (2004) classification (Fig. S3 and Table S3). The Adriatic Basin comprises region DJ3 (Adriatic South); the Ionian Basin comprises regions DJ5, DJ7, and DJ8 (Ionian South, Ionian Middle West, and Ionian Middle East, respectively); the Cretan Passage region comprises region DH3 (Cretan Passage), and the Levantine Basin comprises regions DL1, DL2, DL3, and DL4 (Levantine North, Levantine North-East, Levantine South, and Levantine South-East, respectively). Cruises can be identified with the cruise number in Table 1 and S2. Variables are total alkalinity (TA in µmol kg^{-1}), pH on the total hydrogen ion scale at 25ºC (pH), and total dissolved inorganic carbon (DIC in µmol kg-1). Black dots correspond to the original data, red circles are bias-corrected data.

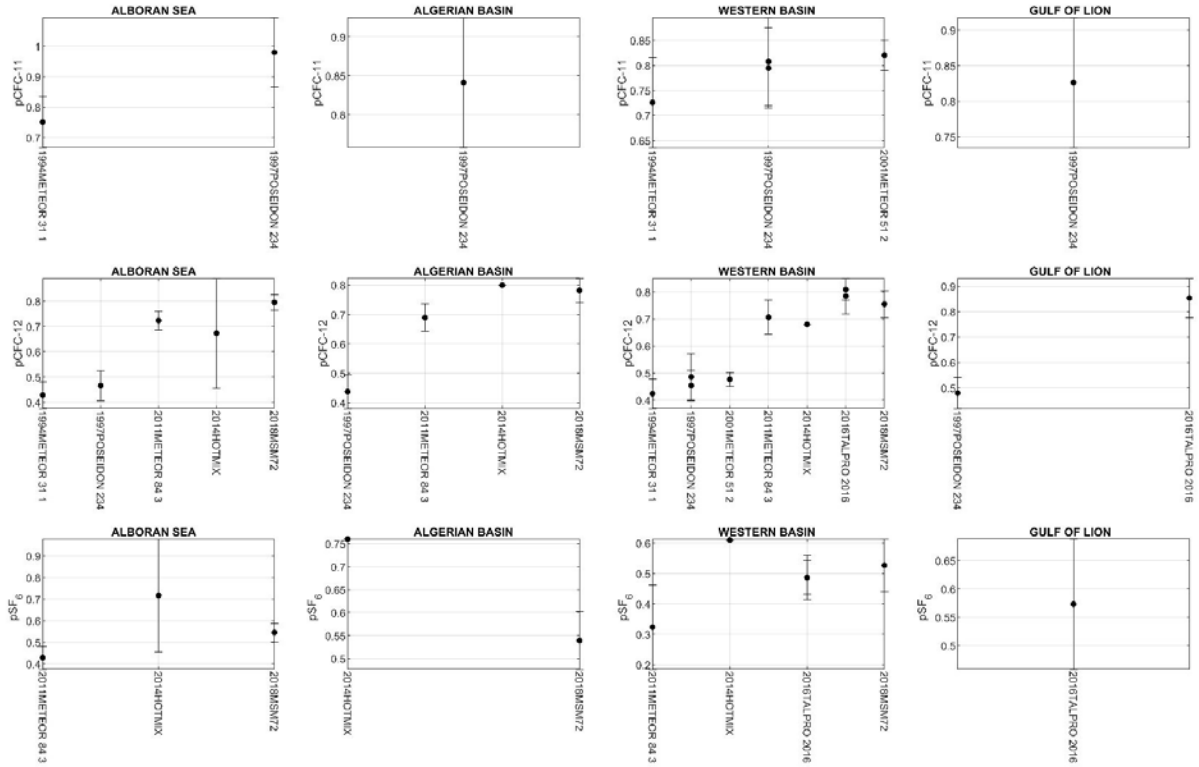

Figure S15. Mean and standard deviation values for the partial pressure of CFC-11, CFC-12, and SF6 (all in ppt), calculated for the depth layers with minimum temporal variability (Section 5.1), CARIMED cruise and Mediterranean Sea grouped sub-basin regions according to Manca et al. (2004) classification (Fig. S3 and Table S3). The Alboran Sea comprises region DS1; the Algerian Basin comprises region DS3 (Algerian West); the Western Basin comprises regions DF1 (Algero-Provençal) and DS1 (Alboran Sea) and the Gulf of Lion comprises region DF2.

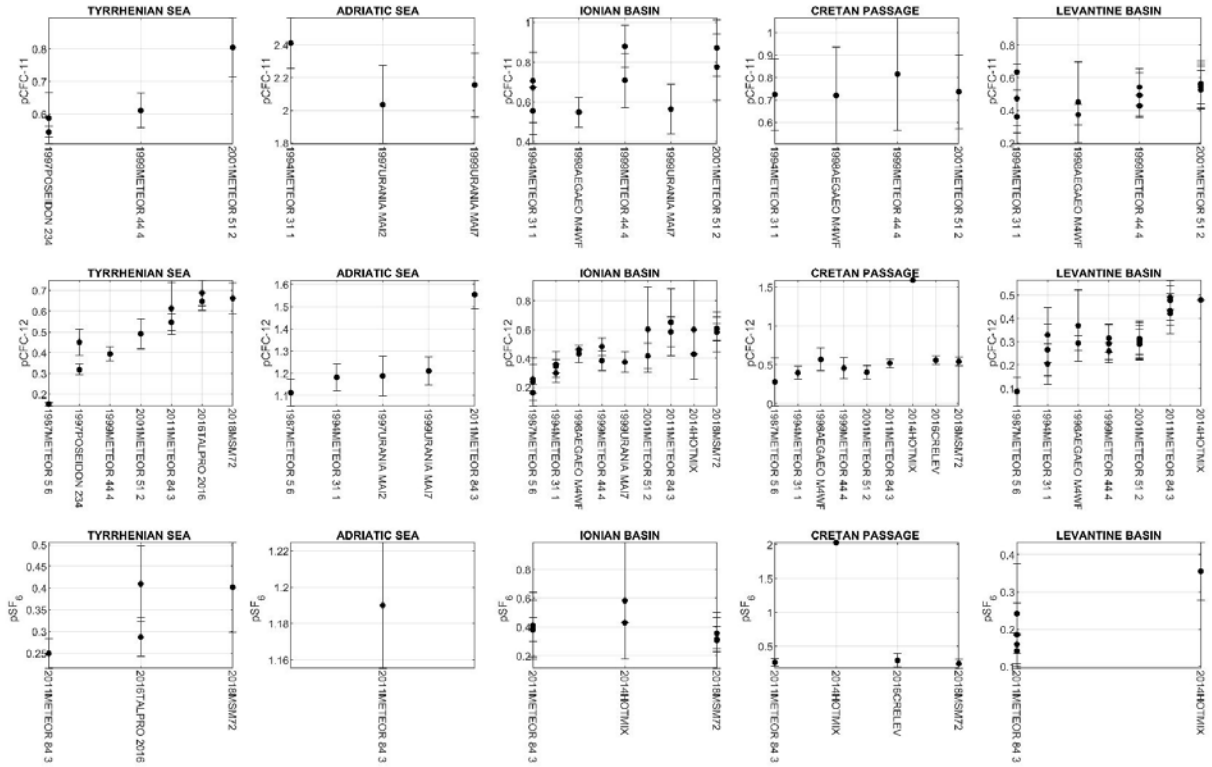

Figure S16. Mean and standard deviation values for the partial pressure of CFC-11, CFC-12, and SF6 (all in ppt), calculated for the depth layers with minimum temporal variability (Section 5.1), CARIMED cruise and Mediterranean Sea grouped sub-basin regions according to Manca et al. (2004) classification (Fig. S3 and Table S3). The Tyrrhenian Basin comprises regions DT1 (Tyrrhenian North) and DT3 (Tyrrhenian South); the Adriatic Basin comprises region DJ3 (Adriatic South); the Ionian Basin comprises regions DJ5, DJ7, and DJ8 (Ionian South, Ionian Middle East, and Ionian West, respectively); the Cretan Passage region comprises region DH3 (Cretan Passage), and the Levantine Basin comprises regions DL1, DL2, DL3, and DL4 (Levantine North, Levantine North-East, Levantine South, and Levantine South-East, respectively).

Table S1. Variable names in the CARIMED original cruise data files along with their corresponding header, units, and flag headers. Individual cruise files are formatted to WHP Exchange Format providing data and metadata in a comma delimited file available in the CARIMED OCADS site.

Variable	Header	Units	Flag Header
Expedition code	EXPOCODE		
Station	STNNBR		
Cast	CASTNO		
Niskin Bottle	SAMPNO		
Date (YYYYMMDD)	DATE		
Hour (HHMM)	TIME		
Latitude	LATITUDE	Decimal degree	
Longitude	LONGITUDE	Decimal degree	
CTD Pressure	CTDPRS	Decibar	
CTD Temperature (ITS-90)	CTDTMP	Degree Celsius	
CTD Salinity (PSS-78)	CTDSAL		CTDSAL_FLAG_W
Salinometer Salinity (PSS-78)	SALNTY		SALNTY_FLAG_W
CTD Oxygen	CTDOXY	µmol kg^{-1}	CTDOXY_FLAG_W
Winkler Oxygen	OXYGEN	µmol kg^{-1}	OXYGEN_FLAG_W
Silicate	SILCAT	µmol kg^{-1}	SILCAT_FLAG_W
Nitrate+Nitrite	NITRAT	µmol kg^{-1}	NITRAT_FLAG_W
Nitrite	NITRIT	µmol kg^{-1}	NITRIT_FLAG_W
Phosphate	PHSPHT	µmol kg^{-1}	PHSPHT_FLAG_W
Total Dissolved Inorganic Carbon	TCARBN	µmol kg^{-1}	TCARBN_FLAG_W
Total Alkalinity	ALKALI	µmol kg^{-1}	ALKALI_FLAG_W
pH on the total hydrogen ion scale at 25ºC and 0 dbar of pressure	PH_TOT_25C		PH_TOT_25C_FLAG_W
Chlorofluorocarbon 11	CFC-11	pmol kg^{-1}	CFC-11_FLAG_W
Chlorofluorocarbon 12	CFC-12	pmol kg^{-1}	CFC-12_FLAG_W
Chlorofluorocarbon 113	CFC-113	pmol kg^{-1}	CFC113_FLAG_W
Sulfur hexafluoride	SF6	fmol kg^{-1}	SF6_FLAG_W
Carbon tetrachloride	CCL4	pmol kg^{-1}	CCL4_FLAG_W
Tritium (^{3}H)	TRITUM	TU	TRITUM_FLAG_W
^{3}H counting error	TRITER	TU	
Helium (He)	HELIUM	nmol kg^{-1}	HELIUM_FLAG_W
He counting error	HELIER	nmol kg^{-1}	
δ^3He	DELHE3	%	DELHE3_FLAG_W
δ^3He counting error	DELHER	%	
Neon (Ne)	NEON	nmol kg^{-1}	NEON_FLAG_W
Ne counting error	NEONER	nmol kg^{-1}	

Table S2. CARIMED cruise summary table with the cruise number, year, EXPOCODE, cruise alias, and DOI (cruise data). The assigned cruise number follows the alphabetical ordering of EXPOCODEs.

Cruise #	Year	EXPOCODE	Alias	DOI
1	2018	06M220180302	MSM72	https://doi.org/10.25921/02fs-yt72
2	1987	06MT19870818	METEOR_5_6	https://doi.org/10.7289/v58s4n8g
3	1994	06MT19941230	METEOR_31_1	https://doi.org/10.25921/6k3e-3x27
4	1999	06MT19990410	METEOR_44_4	https://doi.org/10.25921/hn7s-ss77
5	2001	06MT20011018	METEOR_51_2	https://doi.org/10.3334/cdiac/otg.carina_06mt20011018
6	2011	06MT20110405	METEOR_84_3	https://doi.org/10.3334/cdiac/otg.clivar_06mt20110405
7	1996	06PO19960522	POSEIDON_1996	https://doi.org/10.25921/fscp-wn85
8	1997	06PO19971023	POSEIDON_234	https://doi.org/10.25921/f2z2-2437
9	2009	29AH20090310	FAMOSO	https://doi.org/10.25921/ygts-v572
10	2014	29AH20140426	HOTMIX	https://doi.org/10.25921/xj90-7150
11	2013	29AJ20130502	MEDSEA_2013	https://doi.org/10.7289/v5n87832
12	2016	29AJ20160818	TALPRO_2016	https://doi.org/10.25921/8f6a-zq94
13	1983	29GD19830629	PEP83	https://doi.org/10.25921/n816-dy55
14	2008	29GD20080919	SESAME_SPII	https://doi.org/10.25921/0w06-rf56
15	2008	29RZ20080406	SESAME_SPI	https://doi.org/10.25921/qb64-tc92
16	1977	318M19771204	GEOSECS_LEG3	https://doi.org/10.25921/4wfp-mm25
17	1976	31GI19760901	MILLERO_76	https://doi.org/10.25921/88c2-h343
18	1991	35A319910424	ALMOFRONT_LEG1	https://doi.org/10.25921/tez6-cn71
19	2008	35A320080616	BOUM	https://doi.org/10.25921/xtgz-jr54
20	2011	35A320110301	CASCADE	https://doi.org/10.25921/1mbs-5k19
21	2016	35A320160519	MOOSE_GE_2016	https://doi.org/10.25921/mkbt-aj94
22	1999	35HT19990904	PROSOPE	https://doi.org/10.25921/e2jv-9g03
23	1981	35JC19811020	MEDIPROD_IV	https://doi.org/10.25921/h5rx-0t25
24	2012	35LU20120723	MOOSE_GE_2012	https://doi.org/10.25921/xx8w-gz31
25	2013	35LU20130201	DEWEX	https://doi.org/10.25921/eav3-2q34
26	2014	35LU20140704	MOOSE_GE_2014	https://doi.org/10.25921/c430-sp25
27	2010	35TT20100525	MOOSE_GE_2010	https://doi.org/10.25921/1r3e-te72
28	2014	35TT20140814	SOMBA	https://doi.org/10.25921/2ka0-nj81
29	1995	36AE19950209	OTRANTO_5	https://doi.org/10.3334/cdiac/otg.hcmr_otr5_1995
30	1998	36AE19981014	AEGAEO_M4WF	https://doi.org/10.7289/v5s180sx
31	2013	36AE20131004	PERSEUS_2013	https://doi.org/10.25921/jvqg-mv55
32	2016	36AE20160602	CRELEV	https://doi.org/10.25921/c01n-sv64
33	1983	47SK19831005	MC24IS	https://doi.org/10.25921/4a8h-zf31
34	1984	47SK19840522	MC26IS	https://doi.org/10.25921/3j55-0f80
35	1984	47SK19841204	MC30IS	https://doi.org/10.25921/wzex-ef03
36	1987	47SK19870824	POEM05IS	https://doi.org/10.25921/8bh1-tb18
37	1988	47SK19880807	POEM06IS	https://doi.org/10.25921/ts1g-x108
38	2015	48QL20150804	OC_2015	https://doi.org/10.25921/4jxh-q088
39	2007	48UN20070613	TRANSMED_LEGIII	https://doi.org/10.25921/902g-w994
40	1997	48UR19970830	URANIA_MAI2	https://doi.org/10.25921/g4pn-7922
41	1999	48UR19990211	URANIA_MAI7	https://doi.org/10.25921/zft1-g981
42	2007	48UR20070528	TRANSMED_LEGII	https://doi.org/10.25921/1npj-cs69
43	2008	48UR20080215	SESAME_IT01	https://doi.org/10.25921/bzcp-p786
44	2008	48UR20080301	SESAME_IT02	https://doi.org/10.25921/mbxk-he35
45	2008	48UR20080318	SESAME_IT04	https://doi.org/10.25921/fzpc-d148
46	2008	48UR20081007	SESAME_IT07	https://doi.org/10.25921/satj-p906

Table S3. Code names and regional areas defined by Manca et al. (2004), illustrated in Figure S3.

CODE	AREA
DF2	Gulf of Lion
DF3	Liguro Provencal
DF4	Ligurian East
DS2	Balearic Sea
DF1	Algero Provencal
DS1	Alboran Sea
DS3	Algerian West
DS4	Algerian East
DT1	Tyrrhenian North
DT2	Tyrrhenian East
DT3	Tyrrhenian South
DI1	Sardinia Channel
DI3	Sicily Strait
DJ1	Adriatic North
DJ2	Adriatic Middle
DJ3	Adriatic South

CODE	AREA
DJ6	Ionian North-West
DJ4	Ionian North-East
DJ7	Ionian Middle-West
DJ8	Ionian Middle-East
DJ5	Ionian South
DH1	Aegean North
DH2	Aegean South
DH3	Cretan Passage
DL1	Levantine North
DL2	Levantine North-East
DL3	Levantine South
DL4	Levantine South-East
ATL1	Gulf Cadiz
ATL2	Atlantic

Table S4. Adjustment table for CARIMED cruises, corrections are additive for CTDSAL, TCARBN, ALKALI, and PH_TOT_25C, and multiplicative for OXYGEN, NITRAT, PHSPHT, and SILCAT. Cruises are identified with the cruise number, alias, and EXPOCODE as in Tables 1 and S1. NaN indicates that the variable was not measured in the corresponding cruise and -888 indicates that no 2QC was possible. The CARIMED adjustment workbench is hosted in GEOMAR (https://carimed.geomar.de/).

Cruise #	ALIAS	EXPOCODE	CTDSAL	OXYGEN	NITRAT	PHSPHT	SILCAT	TCARBN	ALKALI	PH_TOT_25C
1	MSM72	06M220180302	0	0%	0%	0%	0%	0	0	0
2	METEOR_5_6	06MT19870818	0	2%	0%	-30%	-10%	NaN	NaN	NaN
3	METEOR_31_1	06MT19941230	0	-5%	0%	49%	0%	NaN	NaN	NaN
4	METEOR_44_4	06MT19990410	0	3%	0%	5%	0%	NaN	NaN	NaN
5	METEOR_51_2	06MT20011018	0	0%	0%	0%	0%	0	5	NaN
6	METEOR_84_3	06MT20110405	0	0%	0%	0%	0%	0	0	0
7	POSEIDON_1996	06PO19960522	-888	NaN	NaN	NaN	NaN	NaN	NaN	NaN
8	POSEIDON_234	06PO19971023	-0.007	NaN	NaN	NaN	NaN	NaN	NaN	NaN
9	FAMOSO	29AH20090310	0	0%	-10%	-12%	0%	NaN	0	0
10	HOTMIX	29AH20140426	0	0%	0%	0%	0%	0	0	0
11	MEDSEA_2013	29AJ20130502	0.01	0%	0%	7%	60%	0	0	NaN
12	TALPRO_2016	29AJ20160818	0	0%	-4%	-5%	-5%	0	0	0
13	PEP83	29GD19830629	0	0%	30%	0%	30%	NaN	0	0
14	SESAME_SPII	29GD20080919	0	0%	0%	0%	0%	NaN	-20	0
15	SESAME_SPI	29RZ20080406	-888	-888	-888	-888	-888	NaN	-888	-888
16	GEOSECS_LEG3	318M19771204	0	0%	0%	0%	0%	0	-20	NaN
17	MILLERO_76	31GI19760901	0	NaN	NaN	NaN	NaN	NaN	-70	0
18	ALMOFRONT_LEG1	35A319910424	0	0%	0%	0%	0%	NaN	0	0
19	BOUM	35A320080616	0	0%	-10%	0%	0%	-10	0	NaN
20	CASCADE	35A320110301	0	0%	-5%	-3%	0%	-10	0	NaN
21	MOOSE_GE_2016	35A320160519	0	0%	0%	0%	0%	0	0	NaN
22	PROSOPE	35HT19990904	0	0%	0%	-50%	0%	NaN	0	0
23	MEDIPROD_IV	35JC19811020	0	0%	0%	0%	0%	0	0	NaN
24	MOOSE_GE_2012	35LU20120723	0	0%	0%	0%	0%	0	0	NaN
25	DEWEX	35LU20130201	0	0%	0%	0%	0%	0	0	NaN
26	MOOSE_GE_2014	35LU20140704	0	0%	0%	0%	0%	0	-10	NaN
27	MOOSE_GE_2010	35TT20100525	0	0%	0%	0%	0%	0	0	NaN
28	SOMBA	35TT20140814	0	0%	0%	0%	-10%	0	-10	NaN
29	OTRANTO_5	36AE19950209	0	0%	2%	0%	2%	-110	140	NaN
30	AEGAEO_M4WF	36AE19981014	0	0%	NaN	NaN	NaN	NaN	NaN	NaN
31	PERSEUS_2013	36AE20131004	-888	-888	-888	-888	-888	-888	-888	-888

32	CRELEV	36AE20160602	0	0%	20%	-15%	15%	15	-777	0
33	MC24IS	47SK19831005	-0.015	-4%	-15%	-14%	10%	NaN	5	0
34	MC26IS	47SK19840522	0	-2%	-20%	-30%	-7%	NaN	12	-888
35	MC30IS	47SK19841204	0	-4%	-25%	0%	0%	NaN	0	0
36	POEM05IS	47SK19870824	0	2%	-15%	NaN	-30%	NaN	0	0
37	POEM06IS	47SK19880807	0	0%	NaN	NaN	NaN	NaN	30	-888
38	OC_2015	48QL20150804	-0.01	0%	0%	0%	0%	NaN	0	0
39	TRANSMED_LEGIII	48UN20070613	0	0%	10%	0%	0%	NaN	10	0
40	URANIA_MAI2	48UR19970830	0	NaN	NaN	NaN	NaN	NaN	NaN	NaN
41	URANIA_MAI7	48UR19990211	0	NaN	NaN	NaN	NaN	NaN	NaN	NaN
42	TRANSMED_LEGII	48UR20070528	0	0%	0%	0%	0%	NaN	6	0
43	SESAME_IT01	48UR20080215	0	-2%	20%	10%	0%	NaN	0	0
44	SESAME_IT02	48UR20080301	0	0%	10%	-15%	-8%	NaN	0	0
45	SESAME_IT04	48UR20080318	0	0%	-10%	0%	0%	0	0	NaN
46	SESAME_IT07	48UR20081007	0	0%	0%	-10%	-15%	NaN	0	0

References

Manca, M., Burca, M., Giorgetti, A., Coatanoan, C., Garcia, M.-J., and Iona, A.: Physical and biochemical averaged vertical profiles in the Mediterranean regions: an important tool to trace the climatology of water masses and to validate incoming data from operational oceanography, J. Mar. Syst., 48, 83-116, doi:10.1016/j.jmarsys.2003.11.025, 2004.